Obatoclax overcomes resistance to cell death in aggressive thyroid carcinomas by countering *Bcl2a1* and *Mcl1* overexpression

Devora Champa, Marika A Russo, Xiao-Hui Liao[1], Samuel Refetoff[1,2], Ronald A Ghossein[3] and Antonio Di Cristofano

Department of Developmental and Molecular Biology, Albert Einstein College of Medicine, Price Center for Genetic and Translational Medicine, 1301 Morris Park Avenue, Room 302, Bronx, New York 10461, USA
Departments of [1]Medicine [2]Pediatrics and Committee on Genetics, University of Chicago, Chicago, Illinois, USA
[3]Department of Pathology, Memorial Sloan-Kettering Cancer Center, New York, New York, USA

Correspondence should be addressed to A Di Cristofano
Email antonio.dicristofano@einstein.yu.edu

Abstract

Poorly differentiated tumors of the thyroid gland (PDTC) are generally characterized by a poor prognosis due to their resistance to available therapeutic approaches. The relative rarity of these tumors is a major obstacle to our understanding of the molecular mechanisms leading to tumor aggressiveness and drug resistance, and consequently to the development of novel therapies. By simultaneously activating *Kras* and deleting *p53* (*Trp53*) in thyroid follicular cells, we have generated a novel mouse model that develops papillary thyroid cancer invariably progressing to PDTC. In several cases, tumors further progress to anaplastic carcinomas. The poorly differentiated tumors are morphologically and functionally similar to their human counterparts and depend on MEK/ERK signaling for proliferation. Using primary carcinomas as well as carcinoma-derived cell lines, we also demonstrate that these tumors are intrinsically resistant to apoptosis due to high levels of expression of the Bcl2 family members, *Bcl2a1* (*Bcl2a1a*) and *Mcl1*, and can be effectively targeted by Obatoclax, a small-molecule pan-inhibitor of the Bcl2 family. Furthermore, we show that Bcl2 family inhibition synergizes with MEK inhibition as well as with doxorubicin in inducing cell death. Thus, our studies in a novel, relevant mouse model have uncovered a promising druggable feature of aggressive thyroid cancers.

Key Words
- thyroid cancer
- mouse model
- cell death

Endocrine-Related Cancer (2014) **21**, 755–767

Introduction

Thyroid cancer is the fifth most prevalent cancer in women, with over 45 000 new cases estimated for 2013 (Siegel *et al.* 2013). Although the vast majority of these tumors are effectively managed by surgical resection followed by radioactive iodine therapy (American Thyroid Association (ATA) Guidelines Taskforce on Thyroid Nodules and Differentiated Thyroid Cancer *et al.* 2009), a subset of lesions, which includes recurring well-differentiated, poorly differentiated, and anaplastic tumors, is refractory to current therapeutic approaches, behaves aggressively, is almost invariably fatal, and thus represents a critical clinical issue (Siironen *et al.* 2010, Ibrahimpasic *et al.* 2013).

http://erc.endocrinology-journals.org
DOI: 10.1530/ERC-14-0268

Published by Bioscientifica Ltd.

Poorly differentiated thyroid tumors have been recently recognized as a defined, although quite heterogeneous, clinical entity, characterized by the presence of a solid, trabecular, or insular growth pattern, absence of conventional nuclear features of papillary carcinoma, and the presence of at least one of the following features: convoluted nuclei, high mitotic activity, or tumor necrosis (Volante *et al*. 2007).

Genetic lesions associated with aggressive poorly differentiated tumors include activation of RAS isoforms and inactivation of p53 (TRP53) (Nikiforov 2004) and, with a lower frequency, activation of BRAF or presence of the RET/PTC rearrangement (Ricarte-Filho *et al*. 2009).

Among the RAS isoforms, *NRAS* represents the most commonly mutated gene (Volante *et al*. 2009), although in a different series *KRAS* was found to be mutated in approximately 45% of all PDTCs analyzed (Garcia-Rostan *et al*. 2003).

Based on these data, we have generated a compound mouse model carrying a constitutively active allele of *Kras* (G12D) and a null *p53* allele. The use of a human thyroid peroxidase promoter-driven Cre recombinase restricts the functionality of the engineered alleles to the thyroid epithelial cells. We show that double-mutant mice invariably develop PDTC in a background of papillary thyroid cancer and that these tumors phenocopy human PDTC and its aggressive behavior. Furthermore, we identify *Bcl2a1* (*Bcl2a1a*) and *Mcl1* as viable therapeutic targets for restoring the sensitivity of mutant cells to drug-induced cell death.

Materials and methods

Animals

The *Kras*^{G12D},*p53*$^{lox/lox}$, and TPO-Cre strains have been described previously (Jonkers *et al*. 2001, Kusakabe *et al*. 2004, Tuveson *et al*. 2004). All strains were backcrossed in the 129Sv background for at least ten generations, and littermates were used as controls.

Hormone measurements

Blood was collected by cardiac puncture. Serum thyroid-stimulating hormone (TSH) was measured using a sensitive, heterologous, disequilibrium double-antibody precipitation RIA (Pohlenz *et al*. 1999), and results were expressed in mU/l. All samples were individually analyzed for each mouse. Total thyroxine (T_4) concentrations were measured by a solid-phase RIA (Coat-a-Count; Diagnostic Products Corp., Los Angeles, CA, USA) adapted for mice. The values of the respective limits of assay sensitivities were assigned to samples with undetectable TSH or T_4 concentrations.

Immunohistochemistry

Sections of 6 μm thickness were subjected to antigen retrieval, incubated with antibodies against thyroglobulin and Ki67 (Dako, Carpinteria, CA, USA), or vimentin, E-cadherin, and pAKT-S473 (Cell Signaling, Danvers, MA, USA), and counterstained with hematoxylin.

Establishment and maintenance of cell lines

Primary thyroid tumors were minced and resuspended in Ham's F12/10% FBS with 100 U/ml type I collagenase (Sigma) and 1 U/ml dispase (Roche). Enzymatic digestion was carried out for 60 min at 37 °C. After digestion, cells were seeded in Ham's F12 containing 40% Nu-Serum IV (Collaborative Biomedical, Bedford, MA, USA), gly–his–lys (10 ng/ml, Sigma), and somatostatin (10 ng/ml, Sigma) and allowed to spread and reach confluence before being passaged. After the fourth passage, tumor cells were adapted to grow in DMEM/10%FBS.

Cal62 cells were grown in RPMI/10%FBS. Identity was validated by amplifying and sequencing genomic fragments encompassing their known mutation (*KRAS* G12R).

Metaphase preparation and chromosome analysis

For chromosome preparation, primary cells at passage p1–p4 were plated in a 35 mm Petri dish and incubated with Colcemid (Sigma–Aldrich) at a concentration of 10 ng/ml overnight or for 3 h at 100 ng/ml. Chromosomes were extracted with standard hypotonic treatment (0.075 M KCl), dropped on microscope slides, and mounted with antifade containing DAPI (Invitrogen). Slides were imaged on a Zeiss Axiovert 200 Microscope using a DAPI filter (Chroma Technologies, Bellows Falls, VT, USA). Ten fields were selected randomly and 15–30 cells for each tumor line were subjected to chromosome counts and visually inspected for the presence of gross chromosome abnormalities and chromosome fragments.

Real-time PCR

Total RNA was extracted with Trizol and reverse transcribed using the Maxima First Strand cDNA Synthesis Kit (Thermo Scientific, Waltham, MA, USA). qRT-PCR was performed on a StepOne Plus apparatus using the Absolute

http://erc.endocrinology-journals.org
DOI: 10.1530/ERC-14-0268

Published by Bioscientifica Ltd.

Blue qPCR Rox Mix (Thermo) and TaqMan expression assays (Applied Biosystems) or the SYBR Green mix (Applied Biosystems) and custom-designed primers (sequences available upon request). Each sample was run in triplicate and *18S* was used to control for input RNA. Data analysis was based on the threshold cycle (Ct) method, and experiments were repeated at least three times using at least two independent organ pools (at least five mice/pool).

Western blot analysis

Cells were homogenized on ice in RIPA buffer supplemented with Complete protease inhibitor tablets (Roche Diagnostics). Western blot analysis was performed on 20–40 μg proteins using phospho-antibodies obtained from Cell Signaling.

Antibody arrays

The Proteome Profiler Human Phospho-Kinase Antibody Array (#ARY003B R&D System, Minneapolis, MN, USA) was probed with extracts from control and GSK1120212-treated cells according to the manufacturer's instructions.

Drug treatments, cell viability, and cell proliferation analysis

GSK1120212 and Obatoclax (Selleck Chemicals, Houston, TX, USA) and doxorubicin (Sigma–Aldrich) were added 24 h after plating, in sextuplicate. After 48–72 h, viability was assessed using the Wst1 assay (Clontech) and IC_{50}s were determined using the Prism software. Alternatively, cells were trypsinized and counted using a Z2 Coulter counter (Beckman Coulter, Indianapolis, IN, USA).

Synergy analysis

Statistical analysis of drug synergy was evaluated from the results of the Wst1 assays and calculated using the Chou–Talalay method (Chou & Talalay 1984) and Compusyn software (www.combosyn.com). To determine synergy between two drugs, the software uses a median-effect method that determines whether the drug combination produces greater effects together than expected from the summation of their individual effects. The combination index (CI) values were calculated for the different dose–effect plots (for each of the serial dilutions) based on the parameters derived from the median-effect plots of the individual drugs or drug combinations at the fixed ratios. The CI was calculated based on the assumption of mutually nonexclusive drug interactions. CI values significantly greater than 1 are antagonistic, not significantly different from one are additive, and values less than 1 are synergistic.

Cell-cycle DNA analysis

Cells were seeded in 10 cm plates, cultured overnight at 37 °C, and incubated for 48 h with GSK1120212 or Obatoclax. Cells were harvested by trypsin treatment and fixed in 75% ethanol on ice. After treatment with RNase, cells were stained with propidium iodide overnight at 4 °C, and the DNA content was measured using a Becton Dickinson LSRII System (BD Biosciences, Franklin lakes, NJ, USA).

Annexin V staining

Cells were seeded in 10 cm plates, cultured overnight at 37 °C, and incubated for 48 h with GSK1120212 or Obatoclax. Cell culture supernatant was collected and added to the cells harvested by trypsin treatment. Cells were stained with Annexin V FITC and PI (BD Pharmigen, Franklin Lakes, NJ, USA) for 15 min at room temperature in the dark. Samples were analyzed by flow cytometry within 1 h using a Becton Dickinson LSRII System (BD Biosciences).

Allograft generation and treatment

WT female 129Sv mice that were 8–10 weeks old received injections of 6×10^6 D445 cells. When tumors reached a size between 100 and 250 mm^3, mice were randomized to placebo, GSK1120212 treatment (1 mg/kg), Obatoclax treatment (4 mg/kg), or combination treatment groups ($n=7$/group). GSK1120212 was administered via oral gavage, and Obatoclax via i.p. injection once every day, and the tumor volume was calculated from two-dimensional measurements using the following equation: tumor volume $=(\text{length}\times\text{width}^2)\times0.5$.

Expression profiling analysis

The dataset GSE27155 was downloaded from the GEO repository and analyzed using GenePattern (Reich *et al.* 2006).

Statistical analysis

Experiments were carried out at least three times. Data were analyzed using the Prism software package.

http://erc.endocrinology-journals.org
DOI: 10.1530/ERC-14-0268

Published by Bioscientifica Ltd.

Differences with P values <0.05 were considered statistically significant.

Results

A novel mouse model of poorly differentiated thyroid cancer

Mice carrying a thyroid-specific deletion of *p53* and expressing the oncogenic *Kras*^{G12D} allele in the thyroid epithelial cells had a median survival of 8.8 months and developed with full penetrance neoplastic lesions starting at 5 months of age (Fig. 1A). Double-mutant mice exhibited a slight decrease in the serum levels of TSH, but no significant alterations in T_4 levels (Table 1). Postmortem analysis of tumor-bearing mice revealed very enlarged glands (207.8±61 vs 18±0.5 mg in WT mice) often tightly adhering to nearby anatomical structures.

Histopathological analysis of the tumors developed by *Kras*^{G12D},*p53*$^{thyr-/-}$ mice indicated that they resemble follicular-cell-derived thyroid carcinomas in humans. Well-differentiated papillary thyroid carcinomas (PTCs) were most prevalent in younger mice and were characterized by papillae and follicle formations, the presence of colloid, low mitotic rate, and absent tumor necrosis (Fig. 1B). Poorly differentiated carcinomas (PDTCs) coexisted with PTCs, displayed organoid growth in the form of solid nests, papillae, or follicles, and exhibited tumor necrosis (often located in the center of the tumor nests) with increased mitotic activity (Fig. 1B). These tumors were often metastatic to the lungs (28% of cases) and displayed elevated staining for the proliferation marker Ki67 (Fig. 1C). Immunostaining for the differentiation marker thyroglobulin showed diffuse labeling in the PTC areas, while the stain labeled only focally the poorly differentiated component (Fig. 1C).

In 40% of mice (six out of 15), tumors contained areas of progression to anaplastic carcinoma, growing in sheets without any organoid formation, composed of markedly pleomorphic spindle or epithelioid cells with very high mitotic activity including atypical mitosis and large areas of tumor necrosis (Fig. 1D). Anaplastic carcinomas did not show any convincing specific staining for thyroglobulin (not shown).

To further characterize the progression from PTC to PDTC and anaplastic thyroid cancer (ATC), we performed

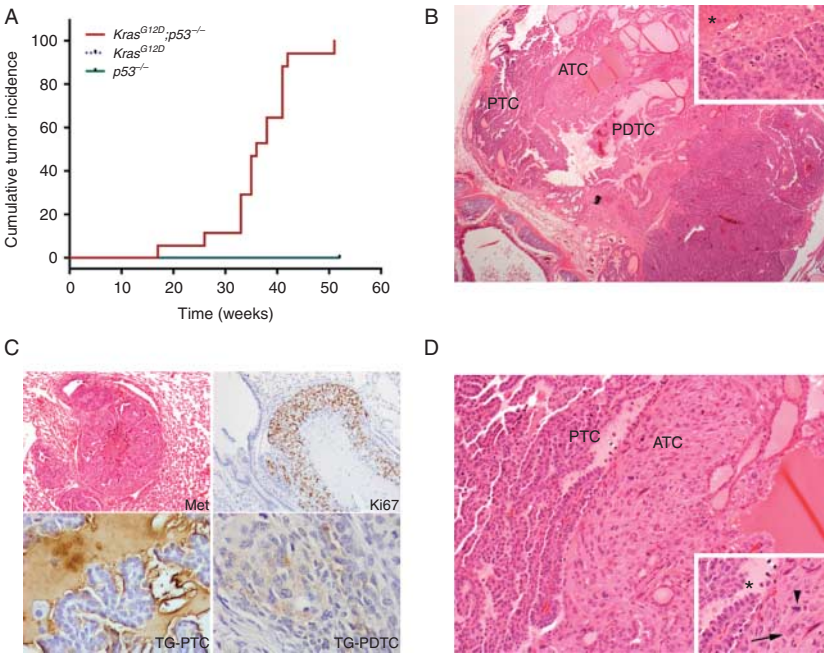

Figure 1

Kras^{G12D},*p53*$^{thyr-/-}$ mice develop papillary thyroid cancer progressing to poorly differentiated and anaplastic carcinomas. (A) Cumulative tumor incidence for mice of the indicated genotypes. (B) Low-magnification (40×) view of a representative tumor showing well-differentiated (PTC), poorly differentiated (PDTC), and anaplastic (ATC) components. The inset (200×) shows a nest of PDTC with adjacent tumor necrosis (asterisk). (C) Top left, PDTC lung metastasis with central tumor necrosis and presence of organoid growth (100×); top right, Ki67 staining showing elevated proliferative index; bottom, immunostaining for thyroglobulin in PTC and PDTC components. (D) Contiguous PTC and ATC (100×); inset: PTC papillae (asterisk), mitotic figure (arrowhead), and anaplastic cells (arrow) (200×). All tumors are from 40- to 50-week-old mice.

http://erc.endocrinology-journals.org
DOI: 10.1530/ERC-14-0268

Published by Bioscientifica Ltd.

Table 1 Hormonal status of control and mutant mice

	WT	$Kras^{G12D}$,$p53^{-/-}$
TSH (mU/l)	336.5±31.5	166.7±46.8
T_4 (μg/dl)	2.40±0.39	2.94±0.36

immunohistochemistry for E-cadherin and vimentin, positive and negative markers of epithelial-to-mesenchymal transition (EMT) respectively. PDTC areas showed a moderate reduction in E-cadherin staining, and no increased vimentin expression, compared with the adjacent PTCs (Fig. 2). Conversely, ATCs showed complete loss of E-cadherin staining and dramatically increased vimentin expression, confirming that these more advanced tumors undergo EMT (Fig. 2). Furthermore, all three histological components (PTC, PDTC, and ATC) of these tumors showed no immunoreactivity for active AKT (pSer473), indicating that the PI3K pathway is not active in tumors driven by Kras activation and p53 loss (Fig. 2).

A frequent aspect of human PDTC and ATC is genomic instability, leading to aneuploidy (Wreesmann *et al.* 2002). We analyzed metaphase spreads from early-passage primary cultures of several tumors developed by $Kras^{G12D}$,$p53^{thyr-/-}$ mice and found that these cultures contained a distinct aneuploid population (Supplementary Figure 1, see section on supplementary data given at the end of this article).

Human PDTC is generally characterized by preserved expression of the *FOXE1*, *PAX8*, and *NKX2-1* transcription factors and the thyroid-specific genes *TSHR*, *TPO*, and *TG*. Expression of *NIS* (*SLC5A5*) is often reduced, leading to refractoriness to radioactive iodine therapy. Complete loss of thyrocyte differentiation is instead a hallmark of human ATC. We used real-time PCR to measure the expression levels of these genes associated with thyroid differentiation and function in freshly dissected glands and tumors. Expression of *Foxe1*, *Pax8*, and *Nkx2-1*, as well as the thyroid-specific genes *Tshr*, *Tpo*, and *Tg*, was generally not altered in single mutants, while the expression levels of *Nis* (*Slc5a5*) were increased in $p53^{-/-}$ glands and reduced in $Kras^{G12D}$ glands (Fig. 3A and B). PDTCs and ATCs retained expression of the thyroid-defining transcription factors and generally showed progressive (less expression with increasing ATC component) loss of *Tpo*, *Tg*, and *Nis* (*Slc5a5*) expression (Fig. 3A and B).

MEK inhibition arrests cell growth without inducing cell death

To aid in the molecular and preclinical characterization of the tumors developed by $Kras^{G12D}$,$p53^{thyr-/-}$ mice, we have established several cell lines from lesions of different prevailing histologies: two of these lines, D316 (PDTC/ATC original tumor) and D445 (PTC/PDTC original tumor), have been used in the experiments described below.

The notion that activation of Kras is the driver oncogenic event for thyrocyte transformation in this model leads to the question of whether these tumors are sensitive to the inhibition of MEK1 and MEK2. We used

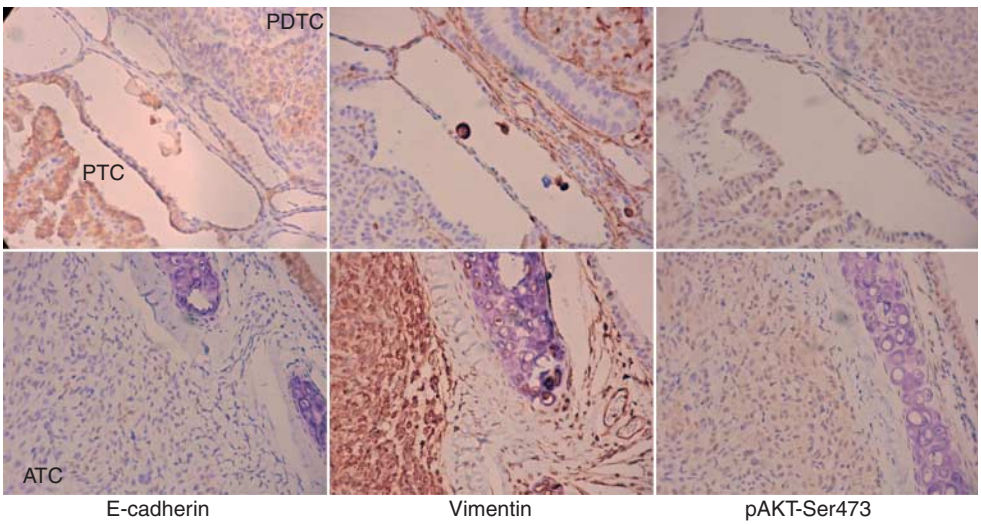

Figure 2
Immunohistochemical detection of E-cadherin, vimentin, and pAKT in PTC, PDTC, and ATC components of the same tumor. Note the progressive loss of E-cadherin, acquisition of vimentin, and absence of activated AKT.

http://erc.endocrinology-journals.org
DOI: 10.1530/ERC-14-0268

Published by Bioscientifica Ltd.

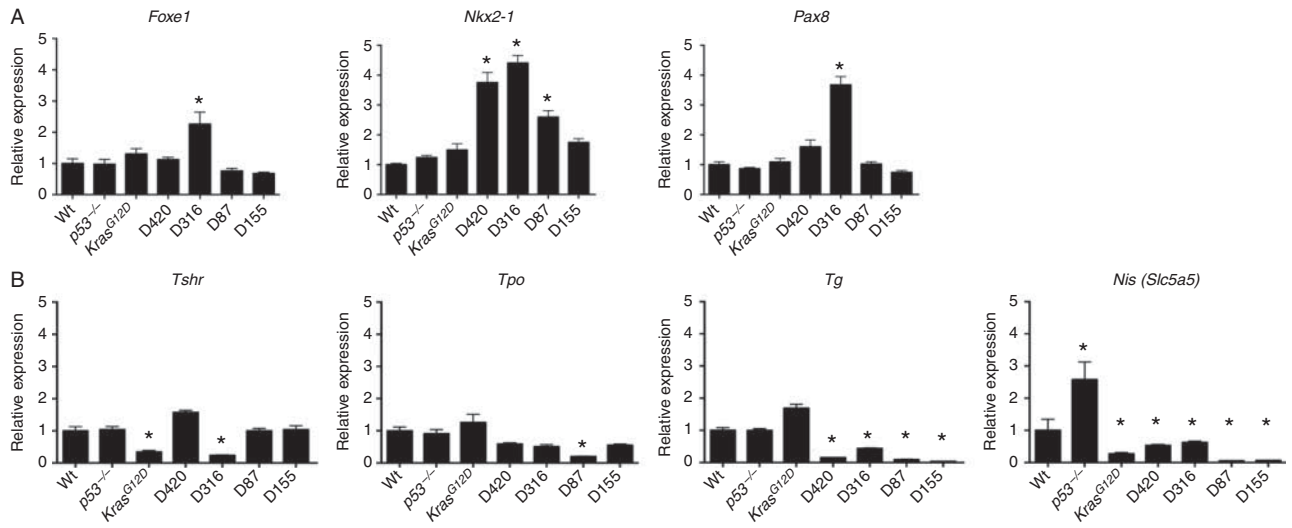

Figure 3

Expression of thyroid specification factors (A) and differentiation/functional (B) markers in $Kras^{G12D}$,$p53^{thyr-/-}$ primary tumors. qPCR on RNA extracted from control and tumor tissues. *$P<0.05$. Tumors are arranged by increasing aggressiveness/dedifferentiation: PTC/PDTC (D316 and D420), and PDTC/ATC (D87 and D155).

two cell lines derived from our mouse model, as well as a human ATC cell line, Cal62, which harbors the same genetic alterations and thus represents an appropriate human counterpart to the mouse lines. These cell lines were treated with the specific MEK1/2 inhibitor GSK1120212 for 72 h to establish a dose–response curve. All three cell lines were effectively growth inhibited in the low nanomolar drug range, with IC_{50}s between 2.5 and 4.5 nM (Fig. 4A).

Growth inhibition was associated with robust cell cycle arrest in the G1 phase in Cal62 cells (Fig. 4B). Although the presence of a significant tetraploid component in the mouse cell lines partially masked this effect (because the G1-arrested tetraploid cells overlap the diploid G2 peak), G1 arrest was also apparent in both D316 and D445 (Fig. 4B).

Importantly, both direct cell counting over several days (not shown) and Annexin V staining of GSK1120212-treated cells showed complete absence of any apoptotic response upon inhibition of the MEK/MAPK pathway in both mouse and human $Kras^{G12D}$,$p53^{-/-}$ cells (Fig. 4C).

We thus tested whether MEK inhibition might result in the activation of feedback loops restoring MAPK phosphorylation or activating compensatory PI3K-mediated pathways in order to support survival in the face of MEK inhibition. Time course analysis of mouse and human cells treated with 100 nM GSK1120212 for up to 48 h did not reveal any restoration of phosphorylated ERK1/2, and no activation of AKT was detectable at any time point (Fig. 4D). We also used an antibody array to interrogate on a larger scale the changes in the phosphokinome of both D316 and Cal62 cells upon GSK1120212 treatment. Besides the expected inactivation of ERK1/2, no significant and consistent GSK1120212-induced changes were detected in either cell lines (Fig. 4E and data not shown). These data strongly indicate that resistance to apoptosis upon inhibition of MEK/MAPK is an intrinsic trait of $Kras^{G12D}$,$p53^{-/-}$ cells and not an adaptive response to MEK inhibition.

$Kras^{mut}$ thyroid tumors overexpress *Bcl2a1* and *Mcl1*

We proposed the hypothesis that the intrinsic resistance to cell death might be associated with altered levels of pro- and anti-apoptotic members of the Bcl2 family. Thus, we measured the expression levels of eight pro-apoptotic and five anti-apoptotic genes in normal thyroid and primary thyroid tumors from $Kras^{G12D}$, $p53^{thyr-/-}$ mice. As shown in Fig. 5, thyroid tumors with varying predominance of the three histological components (PTC, PDTC, and ATC) displayed significantly (at least twofold) elevated mRNA levels for *Bax*, *Bak* (*Bak1*), *Bid*, *Bim* (*Bcl2l11*), *Noxa* (*Pmaip1*), and *Puma* (*Bbc3*), indicating that these tumors are in fact primed to undergo apoptosis. The same trend was observed at the protein level (Fig. 5C). Strikingly, at the same time, these tumors also showed substantial upregulation, both at the RNA and protein levels, of two potent anti-apoptotic genes, *Bcl2a1* and *Mcl1*.

http://erc.endocrinology-journals.org
DOI: 10.1530/ERC-14-0268

Published by Bioscientifica Ltd.

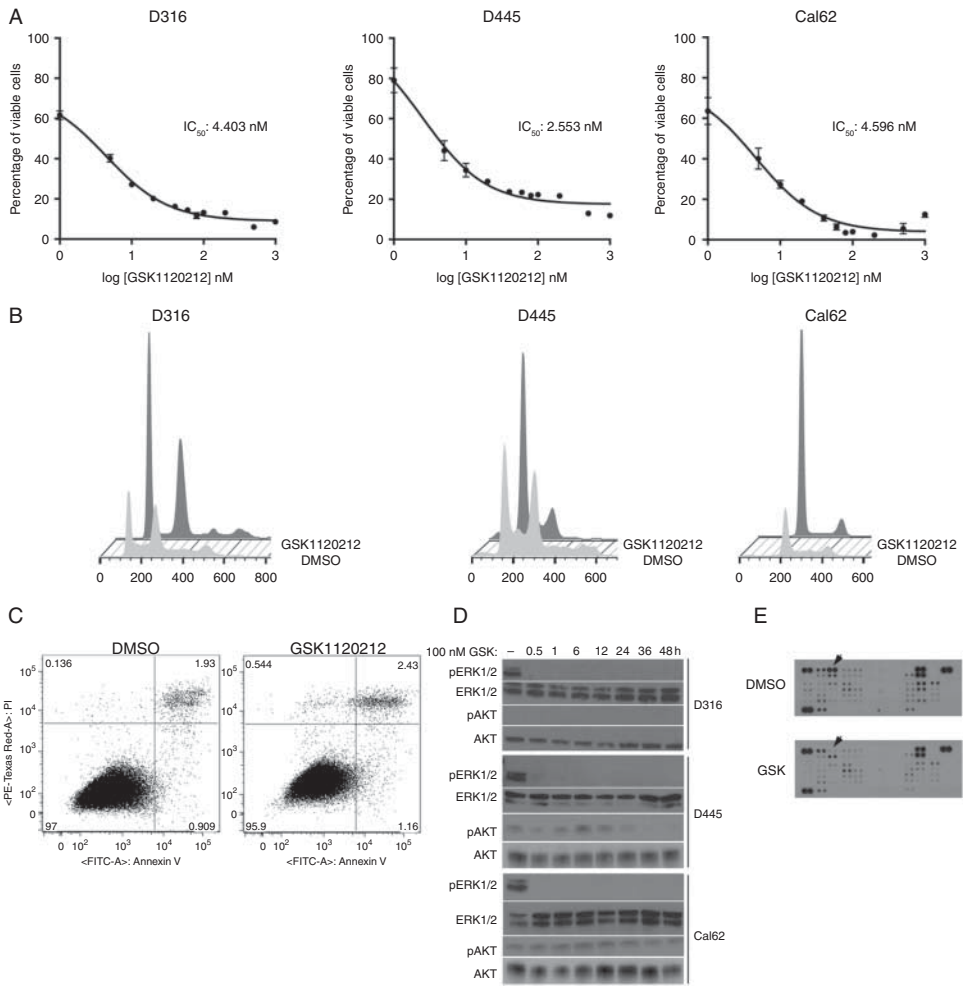

Figure 4

MEK inhibition arrests but does not kill *Kras*^{G12D},*p53*$^{thyr-/-}$ cells. (A) Effect of GSK11201212 on the viability of mouse and human *Kras*^{G12D},*p53*$^{thyr-/-}$ tumor cells. (B) Flow cytometric detection of G1 arrest in MEK-inhibitor-treated cells (dark gray fill) compared with control cells (light gray fill). (C) Flow cytometric detection of apoptotic cells in control and inhibitor-treated D316 cells. Similar results were obtained for D445. (D) Western blot analysis of cells treated with GSK11201212 for the indicated times, showing complete and persistent MEK inhibition and absence of AKT feedback activation. (E) Representative phosphoarray analysis of control and MEK-inhibitor-treated Cal62 cells. Arrows point to pERK1/2. Similar results were obtained using D316 and D445 cells.

A Bcl2 family inhibitor restores cell death response in *Kras*^{mut} tumors

To test whether the high levels of *Bcl2a1* and *Mcl1* protect *Kras*^{G12D},*p53*$^{-/-}$ cells from apoptosis, we used two BH3 mimetic inhibitors, ABT-263 (Tse *et al*. 2008) and Obatoclax (Nguyen *et al*. 2007). ABT-263 targets Bcl2, Bclxl, and Bclw, but not Bcl2a1 or Mcl1, while Obatoclax targets all anti-apoptotic members of the Bcl2 family. ABT-263 was modestly effective in reducing cell viability, while Obatoclax efficiently inhibited cell proliferation in all the three *Kras*^{G12D},*p53*$^{-/-}$ cell lines tested (Fig. 6A), with IC_{50}s in the low nanomolar range. While at lower doses, Obatoclax induced, as shown previously in other cells (Urtishak *et al*. 2013), an accumulation of cells in S-phase without evidence of cell death (Fig. 6B and C), treatment with 500 nM Obatoclax for 48 h induced massive cell death (Fig. 6C). Thus, *Kras*^{G12D},*p53*$^{-/-}$ cells are effectively killed by BH3 mimetics that specifically bind to and inhibit *Bcl2a1* and *Mcl1*.

Then, we tested whether Obatoclax would synergize with inhibition of the RAS/MEK/ERK signaling cascade, which drives these tumors. We compared the single-agent dose–response curves in the mouse cell lines with the curve obtained using the two drugs combined at a fixed

http://erc.endocrinology-journals.org
DOI: 10.1530/ERC-14-0268

Published by Bioscientifica Ltd.

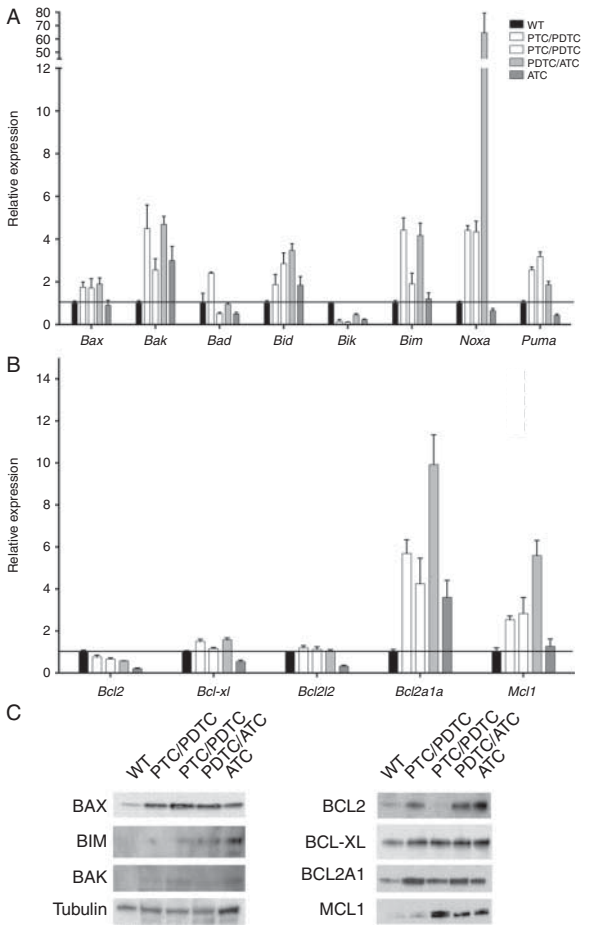

Figure 5
Dysregulation of pro-apoptotic (A) and anti-apoptotic (B) Bcl2 family members in $Kras^{G12D}$,$p53^{thyr-/-}$ primary tumors. qPCR was performed on RNA extracted from tumors with different prevailing histological components. (C) Western blot analysis of the expression of selected pro- and anti-apoptotic proteins in the same tumors used for the RNA analysis above.

ratio based on the most effective single-dose concentration for each drug. The combination treatment was more effective than each single agent over a wide range of concentrations (Fig. 6D). In order to establish whether the combined effects of GSK1120212 and Obatoclax were synergistic rather than additive, we calculated the CI according to the well-established Chou and Talalay median-effect method (Chou & Talalay 1984). The CI for the ED_{95} indicated clearly synergistic effects (CI=0.47).

In order to define the molecular basis for the synergy between MEK1/2 and Bcl2 family inhibition, we determined the changes in expression levels of pro- and anti-apoptotic molecules upon exposure to the inhibitors. GSK1120212 and Obatoclax treatment, alone and in combination, increased the levels of several pro-apoptotic Bcl2 family members (*Bax*, *Noxa*, and *Bim*), thus predisposing the tumor cells to death (Fig. 6E). At the same time, GSK1120212 strongly reduced the expression of *Bcl2a1*, alone and in combination with Obatoclax (Fig. 6F). On the other hand, Obatoclax, as a single agent, increased the expression of most anti-apoptotic Bcl2 family members, probably through a compensatory feedback mechanism. Thus, the synergy between the two compounds is probably obtained through simultaneous upregulation of pro-apoptotic genes, and downregulation and inhibition of anti-apoptotic genes.

The ability of Obatoclax to induce cell death in therapy-resistant cells prompted us to test whether inhibition of *Bcl2a1* and *Mcl1* would sensitize these cells to doxorubicin treatment, which is a current, although poorly effective, standard in advanced thyroid cancer chemotherapy (Shimaoka *et al*. 1985). Indeed, both mouse and human $Kras^{G12D}$,$p53^{-/-}$ cell lines exhibited significantly increased cell death when treated with a combination of GSK1120212 and Obatoclax, than when treated with each compound alone (Fig. 7).

Finally, we used an immunocompetent *in vivo* system, i.e. 129Sv mice bearing D445 allograft tumors, to test the efficacy of Obatoclax as a sensitizer to cell death. Strikingly, the combination of Obatoclax (4 mg/kg) and GSK1120212 (1 mg/kg) resulted in a significant degree of tumor control compared with each drug alone (Fig. 8).

Dysregulation of Bcl2 family members is a feature of human aggressive thyroid carcinomas

We used a large expression-profiling dataset (99 samples) available from the GEO repository (Giordano *et al*. 2005) to test whether the dysregulation of the expression levels of Bcl2 family members observed in our mouse model recapitulates specific human thyroid cancer subtypes. Strikingly, overexpression of *MCL1*, *BCLXL* (*BCL2L1*), and *BID*, and downregulation of *BCL2*, *BAD*, and *BIK* (as observed in the PTCs, PDTCs, and ATCs developed by $Kras^{G12D}$,$p53^{-/-}$ mice) were able to separate classical papillary, tall-cell-variant papillary, and anaplastic carcinomas from all the other subtypes present in the dataset. Additional upregulation of *BCL2A1* and *NOXA* identified a smaller subset of thyroid carcinomas that included all the anaplastic tumors present in the dataset. These results strongly indicate that dysregulation of a set of Bcl2 family

http://erc.endocrinology-journals.org
DOI: 10.1530/ERC-14-0268

Published by Bioscientifica Ltd.

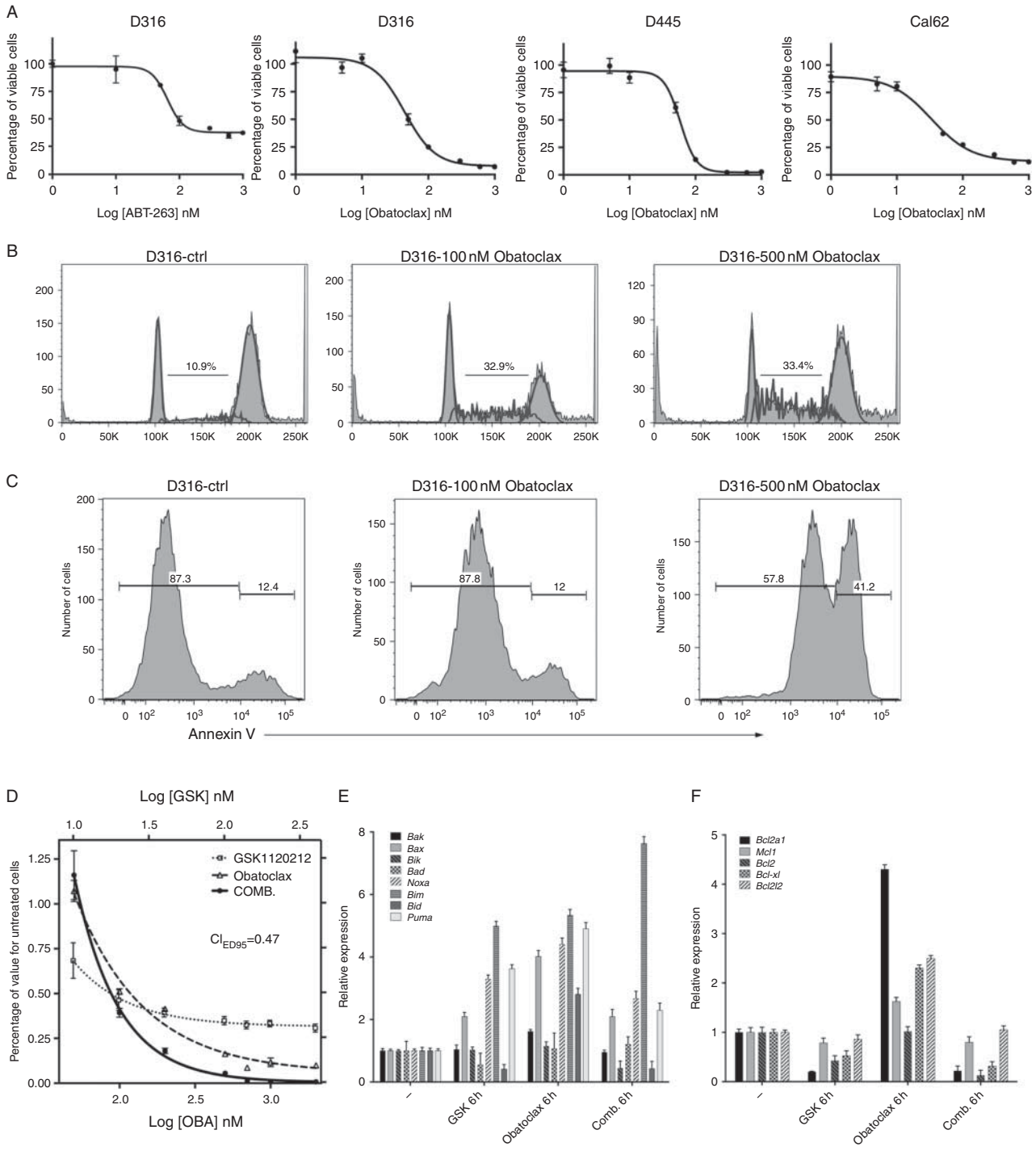

Figure 6

Obatoclax induces cell death in *Kras*^{G12D},*p53*$^{thyr-/-}$ cells and synergizes with MEK inhibition. (A) Effect of ABT-263 and Obatoclax on the viability of tumor cells. (B) Flow cytometric cell cycle analysis of D316 cells treated with 100 and 500 nM Obatoclax. (C) Annexin V staining showing extensive cell death upon treatment of D316 cells with 500 nM Obatoclax. Experiments were replicated with similar results in D445 cells. (D) Dose–response curves showing the cooperative effect of a GSK11201212/Obatoclax combination on the viability of the mouse cell line D445. Drugs were combined at a fixed ratio of 1:5 (GSK/Oba). CI$_{ED95}$: combination index at a drug dose causing 95% reduction in viability. Experiments were replicated with similar results in D316 cells. (E and F) qPCR analysis of the expression of pro- and anti-apoptotic Bcl2 family members in D316 cells upon 6 h treatment with Obatoclax, GSK1120212, and both in combination. Experiments were replicated with similar results in D445 cells.

http://erc.endocrinology-journals.org
DOI: 10.1530/ERC-14-0268

Published by Bioscientifica Ltd.

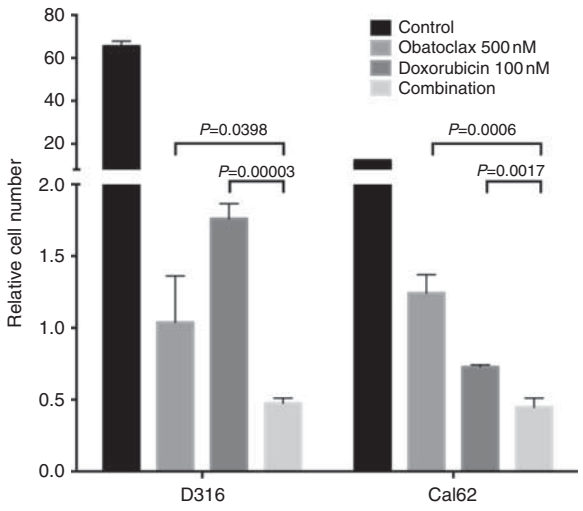

Figure 7
Obatoclax sensitizes $Kras^{G12D}$,$p53^{thyr-/-}$ cells to doxorubicin treatment. The graph shows the number of remaining cells 2 days after treatment with each drug and both in combination, relative to the number of cells plated at the beginning of the experiment.

members, including *MCL1* and *BCL2A1*, identifies thyroid carcinomas with particularly aggressive features (Fig. 9).

Discussion

As for other tumor types, genetically defined murine models of thyroid cancer are invaluable tools to dissect the molecular pathways and events leading to neoplastic transformation and tumor progression, and to test novel, targeted therapeutic approaches in a physiological, immunocompetent system. The past few years have thus seen the generation and exploitation of highly relevant mouse models for follicular (Suzuki *et al.* 2002, Antico-Arciuch *et al.* 2010, Pringle *et al.* 2014), papillary (Jhiang *et al.* 1996, Knauf *et al.* 2005, Chakravarty *et al.* 2011), and ATC (Antico Arciuch *et al.* 2011, Charles *et al.* 2014, McFadden *et al.* 2014). Areas of poor differentiation were observed in advanced papillary tumors developed by $BRAF^{V600E}$ mice (Knauf *et al.* 2011). Herein, we report the generation and characterization of a RAS-driven model that shows progression from papillary lesions to PDTC and, in several cases, to ATC. This model faithfully recapitulates human PDTC, both in terms of morphological and immunohistochemical features, and in terms of genomic instability and tumor aggressiveness. As such, this model represents a valuable tool for identifying key signaling nodes that may allow therapeutic exploitation.

As expected for a model driven by activation of the RAS/MEK/ERK cascade, a MEK inhibitor was able to interfere with tumor cell proliferation. Interestingly, such inhibition was not accompanied by any of the compensatory feedback responses that have been observed in other systems and that can reactivate signaling and proliferation, in particular in *KRAS* mutant tumors (Yoon *et al.* 2010, Turke *et al.* 2012, Carlino *et al.* 2014). However, despite prolonged inhibition of MAPK activity and arrest in G1 phase, tumor cells derived from our mouse model did not undergo cell death, indicating that this system is inherently resistant to apoptosis, similar to the situation observed in human aggressive thyroid tumors, for which cytotoxic therapy often fails. Our data show that the inability to undergo apoptosis, in spite of high levels of expression of pro-apoptotic effectors (*Bak*, *Bid*, *Noxa*, and *Puma*), is at least in part associated with the elevated expression levels of two anti-apoptotic members of the Bcl2 family, *Bcl2a1* and *Mcl1*. *BCL2A1* has been recently described as an oncogene responsible for hematopoietic stem cell transformation (Metais *et al.* 2012) and for resistance to BRAF inhibition in melanoma (Haq *et al.* 2013). The role of *MCL1* in cancer is well established (Ertel *et al.* 2013), and elevated levels of *MCL1* have been reported to correlate with dedifferentiation in thyroid cancer (Branet *et al.* 1996). Accordingly, the pan-Bcl2 family inhibitor Obatoclax, but not the more restricted inhibitor ABT-263, which does not target *Bcl2a1* and *Mcl1*, was able to induce tumor cell death even as a single agent, and to cooperate with MEK inhibition both in cultured

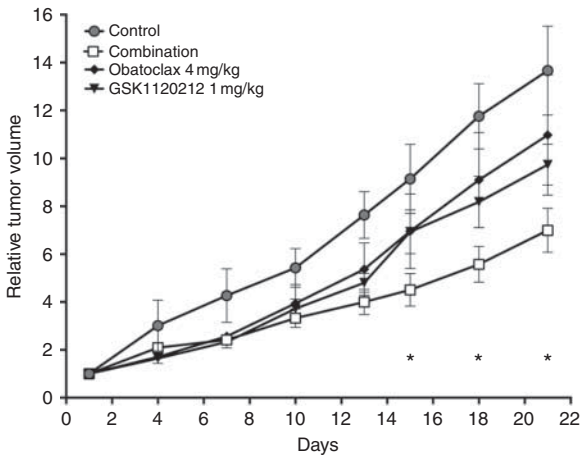

Figure 8
Obatoclax and GSK1120212 activity in a D445 allograft tumor model. Tumor volume was determined every 3 days. Asterisks indicate significant differences between combination and single treatments ($P<0.05$).

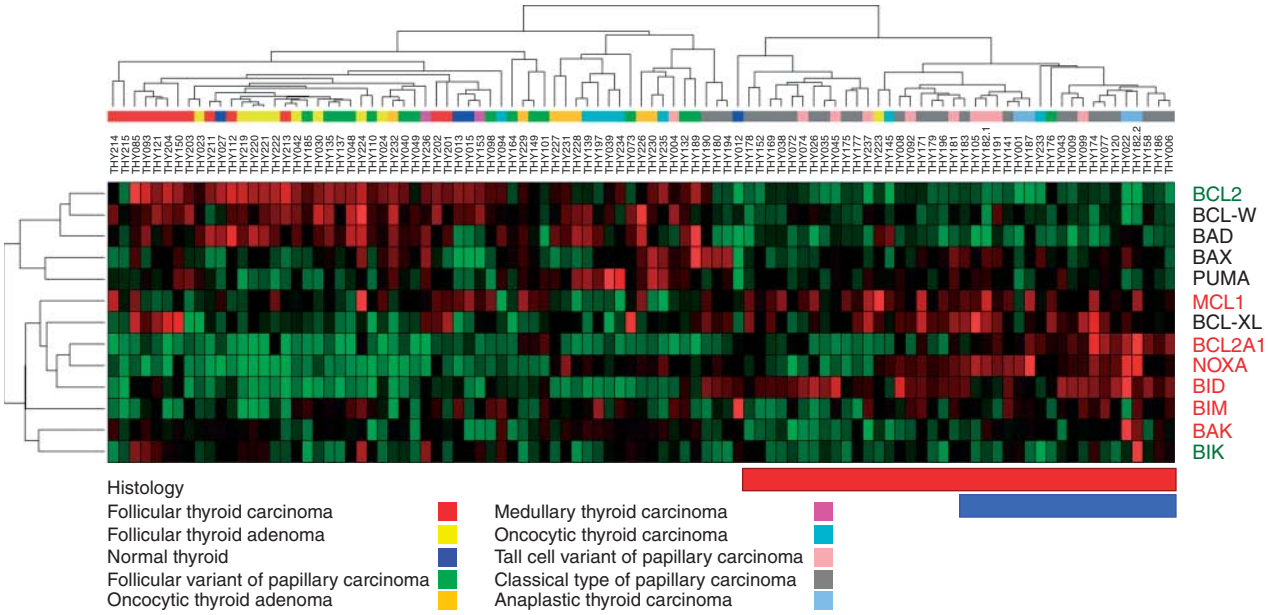

Figure 9

Heat map showing that different subtypes of human thyroid cancer cluster together based on the expression of BCL2 family members. Genes in green are downregulated and genes in red are upregulated in the mouse model. The red bar below the heat map indicates tumors overexpressing MCL1, and the blue bar indicates tumors overexpressing both MCL1 and BCL2A1, as in the mouse model.

cells and, *in vivo*, in tumor cell allografts, as well as with doxorubicin treatment. Thus, targeted inhibition of anti-apoptotic proteins appears to be a valid strategy to sensitize otherwise resistant thyroid cancer cells to cell death induced by inhibition of the driver pathway or cytotoxic chemotherapy. In view of the possible ability of Obatoclax to induce different modes of cell death, including apoptosis, necroptosis, and autophagic death (Heidari *et al*. 2010, Basit *et al*. 2013, Urtishak *et al*. 2013, Yu & Liu 2013), future studies are required to dissect in depth the specific route through which RAS-mutant thyroid cells undergo cell death upon inhibition of anti-apoptotic Bcl2 family members, so that additional fine tuning of the death-inducing system can be achieved for optimal therapeutic responses.

Finally, we have shown that human thyroid cancer subtypes cluster in two main groups based on the expression of BCL2 family members: follicular, follicular variant, and oncocytic carcinomas express high levels of *BCL2* and *BCLW* (*BCL2L2*), and thus may benefit from the sensitizing action of inhibitors such as ABT-263. Classic papillary, as well as the more aggressive tall-cell and anaplastic carcinomas, overexpress *MCL1*, *BCLXL*, and *BCL2A1*, and thus are more sensitive to the inhibitory activity of Obatoclax and its derivatives.

Thus, using a novel mouse model of progression from PTC to PDTC and ATC, as well as a genetically corresponding human cell line, we have uncovered a novel strategy to target thyroid cancer cells for death.

Supplementary data

This is linked to the online version of the paper at http://dx.doi.org/10.1530/ERC-14-0268.

Declaration of interest

The authors declare that there is no conflict of interest that could be perceived as prejudicing the impartiality of the research reported.

Funding

This work was supported by the Albert Einstein Cancer Center Core Grant, and by National Institutes of Health (NIH) grants CA128943 and CA167839 to A Di Cristofano. S Refetoff was supported by grant R37DK15070 from the NIH and the Seymour Abrams fund. A Di Cristofano was a recipient of the Irma T. Hirschl Career Scientist Award.

References

American Thyroid Association (ATA) Guidelines Taskforce on Thyroid Nodules and Differentiated Thyroid Cancer, Cooper DS, Doherty GM,

Published by Bioscientifica Ltd.

Haugen BR, Kloos RT, Lee SL, Mandel SJ, Mazzaferri EL, McIver B, Pacini F *et al.* 2009 Revised American Thyroid Association management guidelines for patients with thyroid nodules and differentiated thyroid cancer. *Thyroid* **19** 1167–1214. (doi:10.1089/thy.2009.0110)

Antico Arciuch VG, Dima M, Liao XH, Refetoff S & Di Cristofano A 2010 Cross-talk between PI3K and estrogen in the mouse thyroid predisposes to the development of follicular carcinomas with a higher incidence in females. *Oncogene* **29** 5678–5686. (doi:10.1038/onc.2010.308)

Antico Arciuch VG, Russo MA, Dima M, Kang KS, Dasrath F, Liao XH, Refetoff S, Montagna C & Di Cristofano A 2011 Thyrocyte-specific inactivation of *p*53 and *Pten* results in anaplastic thyroid carcinomas faithfully recapitulating human tumors. *Oncotarget* **2** 1109–1126.

Basit F, Cristofanon S & Fulda S 2013 Obatoclax (GX15-070) triggers necroptosis by promoting the assembly of the necrosome on autophagosomal membranes. *Cell Death and Differentiation* **20** 1161–1173. (doi:10.1038/cdd.2013.45)

Branet F, Brousset P, Krajewski S, Schlaifer D, Selves J, Reed JC & Caron P 1996 Expression of the cell death-inducing gene bax in carcinomas developed from the follicular cells of the thyroid gland. *Journal of Clinical Endocrinology and Metabolism* **81** 2726–2730. (doi:10.1210/jcem.81.7.8675602)

Carlino MS, Todd JR, Gowrishankar K, Mijatov B, Pupo GM, Fung C, Snoyman S, Hersey P, Long GV, Kefford RF *et al.* 2014 Differential activity of MEK and ERK inhibitors in BRAF inhibitor resistant melanoma. *Molecular Oncology* **8** 544–554. (doi:10.1016/j.molonc.2014.01.003)

Chakravarty D, Santos E, Ryder M, Knauf JA, Liao XH, West BL, Bollag G, Kolesnick R, Thin TH, Rosen N *et al.* 2011 Small-molecule MAPK inhibitors restore radioiodine incorporation in mouse thyroid cancers with conditional BRAF activation. *Journal of Clinical Investigation* **121** 4700–4711. (doi:10.1172/JCI46382)

Charles RP, Silva J, Iezza G, Phillips WA & McMahon M 2014 Activating BRAF and PIK3CA mutations cooperate to promote anaplastic thyroid carcinogenesis. *Molecular Cancer Research* **12** 979–986. (doi:10.1158/1541-7786.MCR-14-0158-T)

Chou TC & Talalay P 1984 Quantitative analysis of dose–effect relationships: the combined effects of multiple drugs or enzyme inhibitors. *Advances in Enzyme Regulation* **22** 27–55. (doi:10.1016/0065-2571(84)90007-4)

Ertel F, Nguyen M, Roulston A & Shore GC 2013 Programming cancer cells for high expression levels of Mcl1. *EMBO Reports* **14** 328–336. (doi:10.1038/embor.2013.20)

Garcia-Rostan G, Zhao H, Camp RL, Pollan M, Herrero A, Pardo J, Wu R, Carcangiu ML, Costa J & Tallini G 2003 *ras* mutations are associated with aggressive tumor phenotypes and poor prognosis in thyroid cancer. *Journal of Clinical Oncology* **21** 3226–3235. (doi:10.1200/JCO.2003.10.130)

Giordano TJ, Kuick R, Thomas DG, Misek DE, Vinco M, Sanders D, Zhu Z, Ciampi R, Roh M, Shedden K *et al.* 2005 Molecular classification of papillary thyroid carcinoma: distinct *BRAF*, *RAS*, and *RET*/*PTC* mutation-specific gene expression profiles discovered by DNA microarray analysis. *Oncogene* **24** 6646–6656. (doi:10.1038/sj.onc.1208822)

Haq R, Yokoyama S, Hawryluk EB, Jonsson GB, Frederick DT, McHenry K, Porter D, Tran TN, Love KT, Langer R *et al.* 2013 *BCL2A1* is a lineage-specific antiapoptotic melanoma oncogene that confers resistance to BRAF inhibition. *PNAS* **110** 4321–4326. (doi:10.1073/pnas.1205575110)

Heidari N, Hicks MA & Harada H 2010 GX15-070 (obatoclax) overcomes glucocorticoid resistance in acute lymphoblastic leukemia through induction of apoptosis and autophagy. *Cell Death & Disease* **1** e76. (doi:10.1038/cddis.2010.53)

Ibrahimpasic T, Ghossein RM, Carlson DL, Chernichenko N, Nixon I, Palmer FL, Lee NY, Shaha AR, Patel SG, Tuttle RM *et al.* 2013 Poorly differentiated thyroid carcinoma presenting with gross extrathyroidal extension: 1986–2009 Memorial Sloan-Kettering Cancer Center experience. *Thyroid* **23** 997–1002. (doi:10.1089/thy.2012.0403)

Jhiang SM, Sagartz JE, Tong Q, Parker-Thornburg J, Capen CC, Cho JY, Xing S & Ledent C 1996 Targeted expression of the ret/PTC1 oncogene induces papillary thyroid carcinomas. *Endocrinology* **137** 375–378. (doi:10.1210/endo.137.1.8536638)

Jonkers J, Meuwissen R, van der Gulden H, Peterse H, van der Valk M & Berns A 2001 Synergistic tumor suppressor activity of BRCA2 and p53 in a conditional mouse model for breast cancer. *Nature Genetics* **29** 418–425. (doi:10.1038/ng747)

Knauf JA, Ma X, Smith EP, Zhang L, Mitsutake N, Liao XH, Refetoff S, Nikiforov YE & Fagin JA 2005 Targeted expression of $BRAF^{V600E}$ in thyroid cells of transgenic mice results in papillary thyroid cancers that undergo dedifferentiation. *Cancer Research* **65** 4238–4245. (doi:10.1158/0008-5472.CAN-05-0047)

Knauf JA, Sartor MA, Medvedovic M, Lundsmith E, Ryder M, Salzano M, Nikiforov YE, Giordano TJ, Ghossein RA & Fagin JA 2011 Progression of BRAF-induced thyroid cancer is associated with epithelial–mesenchymal transition requiring concomitant MAP kinase and TGFβ signaling. *Oncogene* **30** 3153–3162. (doi:10.1038/onc.2011.44)

Kusakabe T, Kawaguchi A, Kawaguchi R, Feigenbaum L & Kimura S 2004 Thyrocyte-specific expression of Cre recombinase in transgenic mice. *Genesis* **39** 212–216. (doi:10.1002/gene.20043)

McFadden DG, Vernon A, Santiago PM, Martinez-McFaline R, Bhutkar A, Crowley DM, McMahon M, Sadow PM & Jacks T 2014 p53 constrains progression to anaplastic thyroid carcinoma in a *Braf*-mutant mouse model of papillary thyroid cancer. *PNAS* **111** E1600–E1609. (doi:10.1073/pnas.1404357111)

Metais JY, Winkler T, Geyer JT, Calado RT, Aplan PD, Eckhaus MA & Dunbar CE 2012 BCL2A1a over-expression in murine hematopoietic stem and progenitor cells decreases apoptosis and results in hematopoietic transformation. *PLoS ONE* **7** e48267. (doi:10.1371/journal.pone.0048267)

Nguyen M, Marcellus RC, Roulston A, Watson M, Serfass L, Murthy Madiraju SR, Goulet D, Viallet J, Belec L, Billot X *et al.* 2007 Small molecule obatoclax (GX15-070) antagonizes MCL-1 and overcomes MCL-1-mediated resistance to apoptosis. *PNAS* **104** 19512–19517. (doi:10.1073/pnas.0709443104)

Nikiforov YE 2004 Genetic alterations involved in the transition from well-differentiated to poorly differentiated and anaplastic thyroid carcinomas. *Endocrine Pathology* **15** 319–327. (doi:10.1385/EP:15:4:319)

Pohlenz J, Maqueem A, Cua K, Weiss RE, Van Sande J & Refetoff S 1999 Improved radioimmunoassay for measurement of mouse thyrotropin in serum: strain differences in thyrotropin concentration and thyrotroph sensitivity to thyroid hormone. *Thyroid* **9** 1265–1271. (doi:10.1089/thy.1999.9.1265)

Pringle DR, Vasko VV, Yu L, Manchanda PK, Lee AA, Zhang X, Kirschner JM, Parlow AF, Saji M, Jarjoura D *et al.* 2014 Follicular thyroid cancers demonstrate dual activation of PKA and mTOR as modeled by thyroid-specific deletion of *Prkar1a* and *Pten* in mice. *Journal of Clinical Endocrinology and Metabolism* **99** E804–E812. (doi:10.1210/jc.2013-3101)

Reich M, Liefeld T, Gould J, Lerner J, Tamayo P & Mesirov JP 2006 GenePattern 2.0. *Nature Genetics* **38** 500–501. (doi:10.1038/ng0506-500)

Ricarte-Filho JC, Ryder M, Chitale DA, Rivera M, Heguy A, Ladanyi M, Janakiraman M, Solit D, Knauf JA, Tuttle RM *et al.* 2009 Mutational profile of advanced primary and metastatic radioactive iodine-refractory thyroid cancers reveals distinct pathogenetic roles for *BRAF*, *PIK3CA*, and *AKT1*. *Cancer Research* **69** 4885–4893. (doi:10.1158/0008-5472.CAN-09-0727)

Shimaoka K, Schoenfeld DA, DeWys WD, Creech RH & DeConti R 1985 A randomized trial of doxorubicin versus doxorubicin plus cisplatin in patients with advanced thyroid carcinoma. *Cancer* **56** 2155–2160. (doi:10.1002/1097-0142(19851101)56:9<2155::AID-CNCR2820560903>3.0.CO;2-E)

Published by Bioscientifica Ltd.

Siegel R, Naishadham D & Jemal A 2013 Cancer statistics, 2013. *CA: A Cancer Journal for Clinicians* **63** 11–30. (doi:10.3322/caac.21166)

Siironen P, Hagstrom J, Maenpaa HO, Louhimo J, Heikkila A, Heiskanen I, Arola J & Haglund C 2010 Anaplastic and poorly differentiated thyroid carcinoma: therapeutic strategies and treatment outcome of 52 consecutive patients. *Oncology* **79** 400–408. (doi:10.1159/000322640)

Suzuki H, Willingham MC & Cheng SY 2002 Mice with a mutation in the thyroid hormone receptor β gene spontaneously develop thyroid carcinoma: a mouse model of thyroid carcinogenesis. *Thyroid* **12** 963–969. (doi:10.1089/105072502320908295)

Tse C, Shoemaker AR, Adickes J, Anderson MG, Chen J, Jin S, Johnson EF, Marsh KC, Mitten MJ, Nimmer P *et al.* 2008 ABT-263: a potent and orally bioavailable Bcl-2 family inhibitor. *Cancer Research* **68** 3421–3428. (doi:10.1158/0008-5472.CAN-07-5836)

Turke AB, Song Y, Costa C, Cook R, Arteaga CL, Asara JM & Engelman JA 2012 MEK inhibition leads to PI3K/AKT activation by relieving a negative feedback on ERBB receptors. *Cancer Research* **72** 3228–3237. (doi:10.1158/0008-5472.CAN-11-3747)

Tuveson DA, Shaw AT, Willis NA, Silver DP, Jackson EL, Chang S, Mercer KL, Grochow R, Hock H & Crowley D 2004 Endogenous oncogenic *K-ras*^{G12D} stimulates proliferation and widespread neoplastic and developmental defects. *Cancer Cell* **5** 375–387. (doi:10.1016/S1535-6108(04)00085-6)

Urtishak KA, Edwards AY, Wang LS, Hudome A, Robinson BW, Barrett JS, Cao K, Cory L, Moore JS, Bantly AD *et al.* 2013 Potent obatoclax cytotoxicity and activation of triple death mode killing across infant acute lymphoblastic leukemia. *Blood* **121** 2689–2703. (doi:10.1182/blood-2012-04-425033)

Volante M, Collini P, Nikiforov YE, Sakamoto A, Kakudo K, Katoh R, Lloyd RV, LiVolsi VA, Papotti M, Sobrinho-Simoes M *et al.* 2007 Poorly differentiated thyroid carcinoma: the Turin proposal for the use of uniform diagnostic criteria and an algorithmic diagnostic approach. *American Journal of Surgical Pathology* **31** 1256–1264. (doi:10.1097/PAS.0b013e3180309e6a)

Volante M, Rapa I, Gandhi M, Bussolati G, Giachino D, Papotti M & Nikiforov YE 2009 RAS mutations are the predominant molecular alteration in poorly differentiated thyroid carcinomas and bear prognostic impact. *Journal of Clinical Endocrinology and Metabolism* **94** 4735–4741. (doi:10.1210/jc.2009-1233)

Wreesmann VB, Ghossein RA, Patel SG, Harris CP, Schnaser EA, Shaha AR, Tuttle RM, Shah JP, Rao PH & Singh B 2002 Genome-wide appraisal of thyroid cancer progression. *American Journal of Pathology* **161** 1549–1556. (doi:10.1016/S0002-9440(10)64433-1)

Yoon YK, Kim HP, Han SW, Oh do Y, Im SA, Bang YJ & Kim TY 2010 *KRAS* mutant lung cancer cells are differentially responsive to MEK inhibitor due to AKT or STAT3 activation: implication for combinatorial approach. *Molecular Carcinogenesis* **49** 353–362. (doi:10.1002/mc.20607)

Yu L & Liu S 2013 Autophagy contributes to modulating the cytotoxicities of Bcl-2 homology domain-3 mimetics. *Seminars in Cancer Biology* **23** 553–560. (doi:10.1016/j.semcancer.2013.08.008)

Received in final form 7 July 2014
Accepted 9 July 2014
Made available online as an Accepted Preprint
10 July 2014

Published by Bioscientifica Ltd.